Journal of Nuclear Materials 379 (2008) 59–67

Contents lists available at ScienceDirect

Journal of Nuclear Materials

journal homepage: www.elsevier.com/locate/jnucmat

Yucca Mountain engineered barrier system corrosion model (EBSCOM)

F. King[a,*], M. Kolar[b], J.H. Kessler[c], M. Apted[d]

[a] *Integrity Corrosion Consulting Ltd., Nanaimo, BC, Canada*
[b] *LS Computing Ltd., Nanaimo, BC, Canada*
[c] *Electric Power Research Institute, Charlotte, NC, USA*
[d] *Monitor Scientific, Denver, CO, USA*

ABSTRACT

A revised engineered barrier system model has been developed by the Electric Power Research Institute to predict the time dependence of the failure of the drip shields and waste packages in the proposed Yucca Mountain repository. The revised model is based on new information on various corrosion processes developed by the US Department of Energy and others and for a 20-mm-thick waste package design with a double closure lid system. As with earlier versions of the corrosion model, the new EBSCOM code produces a best-estimate of the failure times of the various barriers. The model predicts that only 15% of waste packages will fail within a period of 1 million years. The times for the first corrosion failures are 40,000 years, 336,000 years, and 375,000 years for the drip shield, waste package, and combination of drip shield and the associated waste package, respectively.

1. Introduction

In its role in providing an independent scientific analysis of the Yucca Mountain Project (YMP), the Electric Power Research Institute (EPRI) carries out total system performance assessment calculations using the IMARC code [1]. A key input into IMARC is the rate of failure of various components of the engineered barrier system, in particular the titanium drip shield (DS) and Alloy 22 waste package (WP). This paper describes the development of the engineered barrier system (EBS) failure model, referred to as the Engineered Barrier System Corrosion Model (EBSCOM).

EBSCOM predicts the lifetime of the DS and WP as a result of a number of corrosion processes: general corrosion and hydrogen-induced cracking (HIC) of the DS and general corrosion, localised corrosion, microbiologically influenced corrosion (MIC), and stress corrosion cracking (SCC) of the WP. In addition, the possibility that the DS or WP will be improperly emplaced or will contain an undetected manufacturing defect that will result in rapid failure is included in the model.

The EBSCOM code builds on an earlier version of an EPRI EBS model [1] and includes the latest information from corrosion studies from the YMP and elsewhere. A significant improvement in the EBSCOM code is the inclusion of the variability of environmental conditions within the repository. This environmental variability particularly affects the probability of localised corrosion and SCC of the WP as these processes are only possible in a limited number of environments.

Research continues on the corrosion of titanium and Alloy 22 under YM environmental conditions. At the same time, the design of the WP also continues to be optimized. The design and corrosion data presented here represent the status as of 2006–2007, and may not reflect the current design.

2. Treatment of environmental variability in EBSCOM

The nature of the corrosive environment in the drifts is characterised by the variation in temperature and the presence and composition of the aqueous environment.

It is well understood that the drift environment at YM will evolve with time. Three phases of environmental evolution have been defined for the High Temperature Operating Mode (HTOM) [1]:

1. An early dry-out phase persisting for several hundred to several thousand years, during which the drift wall temperature is above boiling. During this period seepage of water onto the EBS will not occur, although deliquescence of soluble salts is possible.
2. An intermediate transition phase extending from the end of the dry-out phase to the time at which initiation of localised corrosion of the WP is no longer possible (7000–8000 years). Both seepage and deliquescence are possible during this phase.
3. A long-term low-temperature phase following the transition period that persists indefinitely. Again, both seepage and deliquescence are possible during this period.

---

* Corresponding author. Tel.: +1 2507511125; fax: +1 2507511884.
E-mail address: fraser.king@shaw.ca (F. King).

0022-3115/$ - see front matter © 2008 Elsevier B.V. All rights reserved.
doi:10.1016/j.jnucmat.2008.06.022

Unlike virtually all of other international repository designs, the Yucca Mountain repository, and the seepage water entering the drifts, are essentially fully aerated at all times. Furthermore, because the combined thickness of the stainless steel transport, aging, and disposal (TAD) container, 316 stainless steel inner vessel, and outer Alloy 22 corrosion barrier is greater than 10 cm, the surface gamma dose rate will be $\ll$1 Gy/h and radiation effects on corrosion will be negligible.

2.1. Variation in temperature and relative humidity

As well as varying in time, the temperature of the EBS varies spatially due to the location in the repository and the disposal of different waste types. Although there is a slight (a few °C) difference in the temperature of the WP and DS, both engineered barriers are assumed to have the same temperature for the purposes of predicting their corrosion performance using EBSCOM. Fig. 1 shows the assumed variation in temperature for the coolest, hottest, and average WP. This range defines the maximum and minimum temperatures in the EBSCOM code. The treatment of the variation in temperature from one EBS to another is discussed in Section 4.2.

As the EBS cools, the relative humidity (RH) in the drift increases. As discussed below, the RH determines not only the composition of deliquescent and evaporating solutions, but also the potential for microbial activity. Fig. 2 shows the predicted variation in RH at the WP surface with temperature [2]. This relationship is used in the EBSCOM code to determine the temperature at which MIC of the WP is possible.

2.2. Composition of the aqueous phase

The composition of the aqueous phase present on the EBS surface, if any, will also vary temporally and spatially. The most concentrated solutions will be present initially, or at least once the surface temperature of the EBS has dropped below the dew point. Deliquescence may occur at temperatures above 100 °C if soluble salts are present on the EBS surface in dust or other deposits. When first formed, deliquescent solutions will be saturated with respect to the dissolved species at a given *T* and RH. As the RH increases, these solutions will become more dilute. Seepage waters that drip onto the EBS during the transition and low-temperature phases may also concentrate by evaporation, the highest concentrations being possible for the hottest EBS temperatures. As with the deliquescent solutions, the concentration of evaporated seepage waters will decrease with time as the temperature drops and the RH increases. For modelling purposes, the composition of the aqueous phase is assumed to be represented by the highest concentration achievable during the evolution of the repository environment.

The composition of seepage waters also varies spatially. Based on the analysis of a large number of pore waters and deliquescent solutions, the US Department of Energy (DOE) has categorised possible waters into 11 classes or 'bins' of common chemical characteristics [3]. The precursor waters for these 11 bins are encountered with varying frequency at YM. The chemical characteristics of these waters determine the nature of the possible corrosion reactions, since not all waters support all DS or WP corrosion mechanisms. For simplicity, EPRI has reduced the number of bins of waters to five (Table 1). As discussed below, localised corrosion and SCC are only possible in certain types of water. The treatment of the variation in the composition of the aqueous phase from one run to another is discussed in Section 4.2.

3. Corrosion processes considered in EBSCOM

A number of WP and DS corrosion processes are considered in EBSCOM for the nominal scenario (i.e., not considering igneous or seismic disruptive events). Other corrosion processes are excluded from consideration by way of reasoned arguments.

3.1. Corrosion of the drip shield

3.1.1. General corrosion

The rate of general corrosion of the DS is given by [1]

$$R_{\mathrm{GC}}^{\mathrm{DS}}(T) = 2f_{\mathrm{F}}R_{\mathrm{GC}}^{\mathrm{DS}}(T_{\mathrm{ref}})\exp\left[\frac{\Delta E_{\mathrm{GC}}^{\mathrm{DS}}}{R}\left[\frac{1}{T_{\mathrm{ref}}}-\frac{1}{T}\right]\right], \tag{1}$$

where $R_{\mathrm{GC}}^{\mathrm{DS}}(T)$ is the rate of general corrosion at temperature *T* (in K), $\Delta E_{\mathrm{GC}}^{\mathrm{DS}}$ is the activation energy, *R* is the gas constant, T_{ref} is the reference temperature for the experimental values of the corrosion rate (348.15 K, 75 °C), f_{F} is an enhancement factor due to the presence of fluoride ions, and the value of 2 accounts for the fact that corrosion can occur on both the top- and under-sides of the DS. The value of the corrosion rate at the reference temperature ($R_{\mathrm{GC}}^{\mathrm{DS}}(T_{\mathrm{ref}})$) is chosen from a cumulative distribution function based on experimental

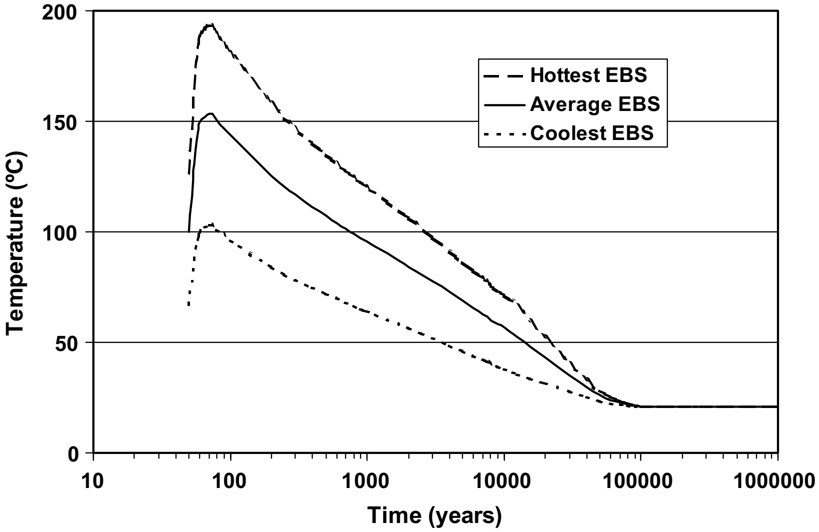

Fig. 1. Assumed variation in temperature for the EBS in the EBSCOM code.

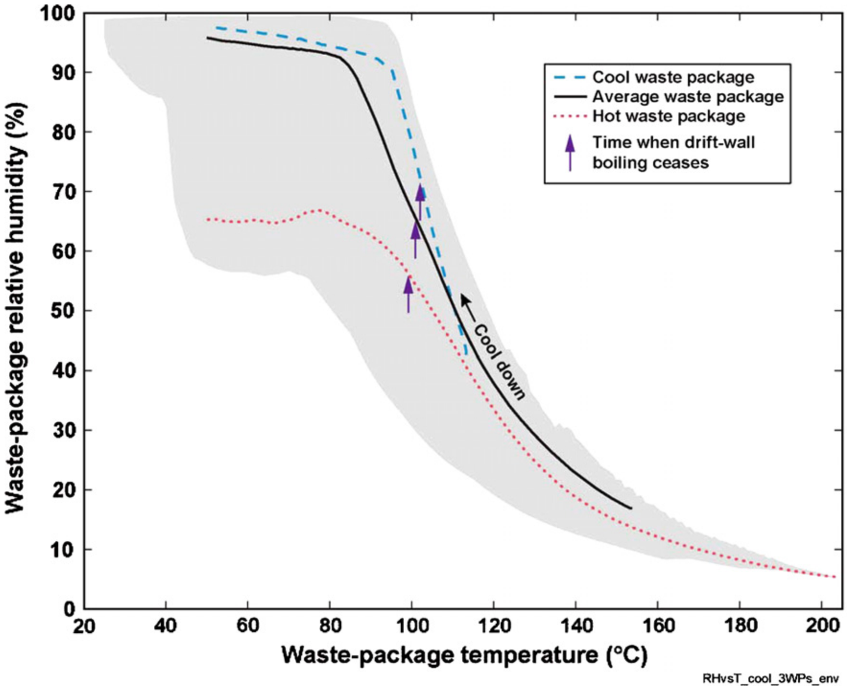

Fig. 2. Predicted variation of the relative humidity at the waste package surface with temperature [2].

Table 1
Classification of seepage and deliquescent waters used in EBSCOM

Bin	End-point brine	Relative frequency (%)
A	K–Ca–Cl–NO_3	1
B	Na–K–Cl–NO_3	17
C	Na–K–Cl	11
D	Na–K–NO_3–Cl	20
E	Na–K–CO_3–Cl	51

measurements [4]. The corrosion rate is assumed to be independent of the environment.

The corrosion rates used to derive the value of $R_{GC}^{DS}(T)$ were obtained with weight-loss samples exposed to various concentrated solutions in the long-term corrosion test facility (LTCTF) for a period of 5 years [4]. These tests showed relatively little effect of the environment on the corrosion rate, and values for the most corrosive solutions were used to develop a Weibull distribution for $R_{GC}^{DS}(T)$, from which a single value is selected for each EBSCOM realisation. The median value of the distribution is equivalent to a corrosion rate of 16 nm/year. Under very specific conditions, fluoride ions have been shown to accelerate the general corrosion of Ti alloys [5]. However, these aggressive low-pH concentrated F^-/Cl^- environments cannot form in most seepage and deliquescent solutions because of the presence of Ca^{2+} (which will lead to the precipitation of F^- ions) and HCO_3^-/CO_3^{2-} (which will buffer the pH in the alkaline range). Accelerated corrosion is particularly unlikely for oxide-covered Ti surfaces, as present on DS exposed to the drift environment for several hundreds or thousands of years prior to the onset of seepage. Nevertheless, a fluoride ion enhancement factor is included in Eq. (1) for the purposes of sensitivity analyses.

3.1.2. Hydrogen induced cracking

The general corrosion of Ti is supported by the reduction of O_2 or H_2O

$$Ti + O_2 + H_2O \rightarrow TiO_2 + H_2O \tag{2a}$$

or

$$Ti + 2H_2O \rightarrow TiO_2 + 4H \tag{2b}$$

Only the corrosion of Ti by H_2O produces hydrogen atoms that can be absorbed by the DS and lead to hydrogen-induced cracking. Failure of the DS by HIC is deemed to occur once the absorbed hydrogen concentration $[H_{ABS}]$ reaches a critical value H_{CRIT} [1].

The rate of H absorption depends on a number of factors [5], including:

1. the rate of general corrosion,
2. the fraction of corrosion supported by the reduction of H_2O,
3. the fraction of H produced by Reaction (2b) that is absorbed by the oxide-covered metal (f_H), and
4. the amount of absorbed H released from the matrix as corrosion proceeds.

Of the total rate of corrosion, a fraction f_{O2} is assumed to be supported by the reduction of O_2 (Reaction (2a)) and a fraction $(1 - f_{O_2})$ by the reduction of H_2O (Reaction (2b)). The fraction of the total corrosion supported by O_2 reduction will be a function of the drift environment. At elevated temperatures the solubility of dissolved O_2 will diminish, an effect that may be compounded by the salting-out of O_2 in concentrated evaporates. At lower temperatures, the solubility of dissolved O_2 is higher, and a larger fraction of the overall corrosion may be supported by Reaction (2a). For simplicity, the value of $1 - f_{O_2}$ is assumed to be independent of temperature and the nature of the solution in the current version of EBSCOM. It should be noted that the LTCTF tests from which the data for $R_{GC}^{DS}(T)$ were taken were conducted under naturally aerated conditions at temperatures of 60 °C and 90 °C. Therefore, the observed corrosion is a result of the cathodic reduction of both O_2 and H_2O. No significant dependence on temperature was found in these tests, although more-recent data have shown a temperature dependence equivalent to an activation energy of ~23 kJ/mol [5].

The absorbed H is assumed to be uniformly distributed throughout the DS. Preferential precipitation of H (as Ti hydrides) is observed during localised corrosion of Ti alloys in regions that are corroding relatively rapidly and for which the protective oxide film is thin or absent due to the low-pH in the pit or crevice. However, for the general corrosion of the DS the assumption of a uniform concentration throughout the structure is reasonable given the relatively slow rate of H absorption compared with the rate of diffusion of H in the Ti matrix.

The conversion of the Ti matrix to TiO_2 can be reasonably expected to release the absorbed H, which is then free to escape into the drift environment [6]. In the EBSCOM code, therefore, it is assumed that H already absorbed is lost as the Ti matrix is converted into TiO_2.

The critical hydrogen concentration for HIC is of the order of 1000 ppmw [6].

3.1.3. Corrosion processes not considered for the drip shield

In the absence of seismically induced deformation and stresses, the DS is assumed to be immune to SCC. Furthermore, Ti-7 is assumed to be immune to MIC [7,8].

3.2. Corrosion of the waste package

In the EBSCOM code, corrosion of the WP is assumed to take the form of general corrosion, localised corrosion, stress corrosion cracking, and microbiologically influenced corrosion.

3.2.1. General corrosion

The rate of general corrosion of the WP ($R_{GC}^{WP}(T)$) is given by an Arrhenius relationship of the form [1]

$$R_{GC}^{WP}(T) = f_{MIC} R_{GC}^{WP}(T_{ref}) \exp\left[\frac{\Delta E_{GC}^{WP}}{R}\left[\frac{1}{T_{ref}} - \frac{1}{T}\right]\right], \tag{3}$$

where f_{MIC} is an enhancement factor for MIC (see Section 3.2.4) and the other terms are analogous to those in Eq. (1). As for the Ti-7 DS, the rate of general corrosion at the reference temperature ($R_{GC}^{WP}(T_{ref})$) is derived from a Weibull fit to 5-year corrosion data from the LTCTF, with a median rate of 9 nm/year at 75 °C [9]. These tests show little effect of the composition of the aqueous phase, so that the same distribution is used in EBSCOM for all possible environments. The activation energy (ΔE_{GC}^{WP}) was derived from linear polarization corrosion rate measurements at various temperatures and has a value of 25.9 kJ/mol [9].

For the laser-peened stress-relieved region of the outer closure lid weld, the rate of general corrosion is further modified by a factor f_{GCLP} to account for the reduction in corrosion rate for laser-peened material [10]. The depth of the laser-peened region is defined as that for which the residual stress is $\leqslant 0$ MPa, i.e., the absence of tensile residual stress. The residual stress is a function of thickness through the weld, as described in Section 3.2.3 below. The factor f_{GCLP} is set to unity if the closure weld is not laser-peened and a uniform distribution of 0.43–0.54 for peened material.

There is contradictory evidence in the literature regarding the effect of thermal ageing on the rate of GC of Alloy 22. Rebak et al. [11] report enhanced corrosion rates of thermally aged material in a highly aggressive industry standard test environment (ASTM G28A, boiling 50% $H_2SO_4 + 42$ g/L $Fe_2(SO_4)_3$). However, tests in environments more relevant to those expected in the repository indicate no such enhancement [4,9]. Therefore, no enhancement factor is included in EBSCOM for the effect of thermal ageing.

3.2.2. Localised corrosion

Localised corrosion of the Alloy 22 WP can occur in some environments, but only if seepage water contacts the waste package and concentrates by evaporation. A pre-requisite for localised corrosion of the WP, therefore, is that the DS has failed. It has been shown that deliquescent solutions that might form due to dust deposits cannot sustain localised corrosion [12]. Localised corrosion of Alloy 22 has been observed in the laboratory in divalent cation (Ca^{2+}, Mg^{2+}) chloride solutions at elevated temperature [4,9,13]. The addition of nitrate, sulphate, and/or carbonate ions to the solution inhibits the initiation of localised corrosion. The majority of seepage and deliquescent solutions that might form on the surface of the WP at Yucca Mountain do not contain the necessary ions to support localised corrosion. In fact, of the various bins of possible seepage waters sampled in EBSCOM, only the Ca-containing Bin A water will support localised corrosion of the WP. This water accounts for only 1% of all of the possible waters at YM.

The EBSCOM code treats both the initiation and propagation of localised corrosion. Initiation is treated using a threshold temperature. Once initiated, localised corrosion is assumed to continue to propagate at a rate that decreases with time.

In a $Ca^{2+}–Cl^{-}–NO_3^{-}$ water that could support localised corrosion, the probability of initiation of localised attack is a complex function of the $[Cl^{-}]$, $[Cl^{-}]:[NO_3^{-}]$, electrochemical potential, and temperature. Since the solution composition changes with time because of the evolution of the temperature and RH in the drift, the conditions for localised corrosion will also change. In order to encompass the complex interdependence of these parameters whilst maintaining a level of simplicity in the EBSCOM code, the threshold condition for the initiation of localised corrosion is reduced to a critical temperature (T_{LC}). Localised attack will not initiate below T_{LC} regardless of the composition of the solution on the WP surface (even in Bin A waters) and regardless of the value of the corrosion potential (E_{CORR}). Microstructural changes introduced during welding increase the susceptibility of Alloy 22 to localised corrosion initiation, so separate T_{LC} are defined in EBSCOM for the WP outer barrier ($T_{LCshell}$) and for the outer and middle closure lid welds (T_{LCweld}).

In summary, therefore, the pre-requisites for localised corrosion of the WP are:

1. the temperature must be $\leqslant T_{AQ}$, the temperature at which a stable aqueous phase can form (this is a pre-requisite for all forms of corrosion of the WP and DS),
2. the selected environment must support localised corrosion (i.e., Bin A water),
3. the drip shield must have failed, and
4. the temperature must be $\geqslant T_{LC}$.

If localised corrosion initiates, it is assumed to continue to propagate indefinitely. However, the rate of propagation decreases with increasing time (and deceasing temperature), essentially stifling growth after a certain period. The rate of propagation R_{LC} is given by the following general fit to experimental data for a range of passive alloys [1],

$$R_{LC} = Bnt^{n-1}, \tag{4}$$

where n is the time exponent for localised corrosion (uniform distribution between 0.1 and 0.5) and B is a temperature-dependent growth constant described by a Weibull distribution with a median value of 54 nm/year [1].

3.2.3. Stress corrosion cracking

In the nominal scenario, SCC only affects the WP closure lid welds. The WP outer barrier (including the non-closure lid) is heat treated to relieve manufacturing stresses prior to encapsulation of the waste fuel. Once filled with the wasteform and sealed, the WP cannot be stress relieved through heat treatment, although the surface of the outer closure lid weld is assumed to be stress relieved by laser-peening or low-plasticity burnishing [10].

Work reported by the DOE [14] and by the Center for Nuclear Waste Regulatory Analyses (CNWRA) [13] has shown that Alloy 22 is highly resistant to crack initiation and growth. The DOE have only observed cracking under certain, very specific, environmental conditions [14], whilst the CNWRA studies show no indications of crack initiation or growth at all. Nevertheless, the possibility of SCC is included in the EBSCOM code and, along with the treatment of other corrosion processes, is based on EPRI's best-estimate of the likely SCC behavior of the WP derived primarily from the data presented by the DOE [14].

In EBSCOM, there are a number of pre-requisites for SCC of the closure lid welds:

1. the environment must support SCC,
2. the value of the corrosion potential E_{CORR} must be equal to or exceed the threshold potential for SCC, and
3. the surface tensile stress in the weld (σ) must exceed the threshold stress for crack initiation (σ_{INIT}).

A fourth criterion for the SCC of the middle closure lid weld is that the outer closure lid must have previously failed, thus permitting an aqueous environment to form on the middle lid weld.

Crack propagation is assumed to be rapid compared with the periods under consideration, so the EBSCOM SCC sub-model is based on a threshold stress initiation criterion. A second initiation criterion will be included in future versions of the model based on the threshold stress intensity factor for SCC (K_{ISCC}), once the actual size and shape of weld defects that might pass inspection are available from WP fabrication trials.

Fig. 3 shows a summary of the DOE slow strain rate test (SSRT) results in a range of environments as a function of the electrochemical potential. In the figure, tests in which SCC was observed are indicated by the full symbols, whereas the absence of SCC is indicated by the open symbols and horizontal lines. The results show that the susceptibility of Alloy 22 to SCC is a function of both the nature of the aqueous environment and of the electrochemical potential. Cracking was only observed in simulated concentrated water (SCW) and then only at relatively positive potentials. Cracking was not observed in simulated acidified water (SAW) with and without the addition of $\text{Pb(NO}_3)_2$, basic saturated water (BSW) (including BSW modified by the removal of sulphate and/or nitrate ions), or simulated saturated water (SSW). These test solutions represent concentrated solutions that might form on the surface of the WP exposed to seepage or deliquescent solutions and which are subsequently concentrated by evaporation. Solutions that might evolve into a concentrated water similar to SCW (i.e., Bins D and E) constitute 71% of the waters simulated by the EBSCOM code (Table 1).

Even if the appropriate environment forms on the WP closure lid welds, cracking is only possible if E_{CORR} is sufficiently positive. Cracking was only observed experimentally at potentials $\geqslant 200\ \text{mV}_{\text{SSC}}$, a potential that is typically 340–620 mV more positive than E_{CORR} [14]. In SCW solutions, E_{CORR} varied between $-241\ \text{mV}_{\text{SSC}}$ and $-76\ \text{mV}_{\text{SSC}}$ in the DOE tests. The triangular border in Fig. 3 represents the range of potentials for which SCC is considered possible in EBSCOM. This region extends to a minimum potential of $0\ \text{mV}_{\text{SSC}}$, 200 mV below the minimum potential for cracking reported to date and, hence, retains a significant degree of conservatism. An asymmetrical triangular distribution is used for the threshold potential for SCC, with upper and lower bounds of $+400\ \text{mV}_{\text{SSC}}$ and $0\ \text{mV}_{\text{SSC}}$, respectively, and a maximum probability of cracking at $+400\ \text{mV}_{\text{SSC}}$. In the model, SCC is only considered possible in the 71% of susceptible sampled waters if the calculated value of E_{CORR} exceeds the threshold potential.

DOE have developed an expression for predicting the value of E_{CORR} based on fitting a range of data to various functional relationships [9]. The function found to best describe the observed dependence of E_{CORR} on temperature (T in °C), pH, and the $[\text{Cl}^-]$ and $[\text{NO}_3^-]$ (in mol kg^{-1}) is

$$E_{\text{CORR}} = c_0 + c_1T + c_2\text{pH} + c_3[\text{Cl}^-] + c_4\log\left(\frac{[\text{NO}_3^-]}{[\text{Cl}^-]}\right). \qquad (5)$$

In EBSCOM, the E_{CORR} for solutions that can support SCC (Bins D and E) is given by

$$E_{\text{CORR}} = -101.82 + 0.677T\ \text{mV}_{\text{SSC}}, \qquad (6)$$

based on a composition of $[\text{Cl}^-] = 1\ \text{mol kg}^{-1}$, $[\text{NO}_3^-]:[\text{Cl}^-] = 1.057$, and pH 10 [3]. The value $-101.82\ \text{mV}_{\text{SSC}}$ is assumed to be normally distributed with a standard deviation of 36.156 mV (as for the coefficient c_0 in Eq. (5) [9]).

The third criterion for SCC is that the surface stress exceed the value of σ_{INIT}. Crack initiation generally requires some degree of plastic deformation, suggesting a threshold stress in the region of the yield stress (YS). This conclusion is confirmed by the results of DOE constant-load tests which showed no crack initiation for loads of up to 2.1YS [14]. Furthermore, plastically deformed Alloy

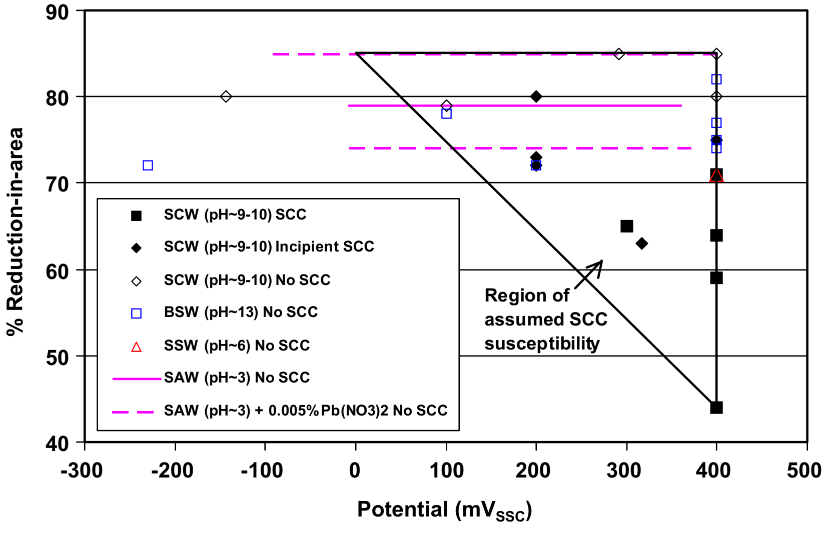

Fig. 3. Summary of the DOE slow strain rate SCC tests as a function of electrochemical potential [14].

22 U-bend specimens have not shown crack initiation after exposure to various concentrated test waters in the LTCTF for periods of up to 5 years. The SSRT described above in which some crack initiation was observed under specific environmental and electrochemical conditions are severe tests in which the sample is tested to failure. Initiation may have occurred at any time during the test but, based on the DOE constant-load and U-bend tests, it is likely to have occurred only after yielding of the sample had commenced. Based on this evidence, the threshold stress for crack initiation in the EBSCOM model is assumed to be given by a uniform distribution with upper and lower bounds of 1.0 YS and 0.9 YS, respectively.

The distribution of residual stresses in the closure welds is required to determine whether the surface stress exceeds the value of σ_{INIT}. For the nominal scenario, the residual stresses in the hoop and radial directions for the outer and middle closure lid welds are provided by DOE [14].

Fig. 4 compares the residual hoop stresses (larger than the equivalent radial component) with the EBSCOM initiation criteria of 0.9–1.0 YS for temperatures of 25 °C and 160 °C. Since the YS increases with decreasing temperature, the probability of crack initiation decreases with increasing time as the repository cools. It is apparent from Fig. 4 that the outer closure lid weld is not susceptible to crack initiation in its pristine state because of the surface compressive stress produced by the laser-peening process. However, as the surface of the weld is corroded by a combination of general and localised corrosion, the sub-surface tensile region may be exposed to the environment. In EBSCOM, it is assumed that the residual stress distribution shown in Fig. 4 remains unchanged as the surface of the weld is corroded. Thus, once the outer 2–3 mm of the outer closure lid weld has been corroded, the surface residual stress changes from compressive to tensile. Once 5–10 mm of the weld has been removed by corrosion, the surface tensile stress may be sufficiently high for crack initiation. This is a conservative assumption since, in reality, the residual stresses will re-distribute as the compressive surface layers are removed and the peak tensile stress would be expected to decrease.

3.2.4. Microbiologically influenced corrosion

Microbiologically influenced corrosion of the WP is potentially important in the long-term once environmental conditions in the drift have ameliorated sufficiently to allow microbial activity. One of the major stressors for microbial activity in the repository is the general lack of water, characterised by the low RH in the drift. The RH is numerically equal to the thermodynamic water activity a_W, a parameter that has been linked to the viability of different types of microbe [15]. Most microbial species are not active at $a_W < 0.96$, and this water activity has been proposed as a threshold value for the modelling of microbial activity in nuclear waste repositories [16]. The time dependence of the RH (or a_W) in the drifts is not explicitly included in EBSCOM but, since RH and temperature are closely linked (Fig. 2), the conditions for the onset of microbial activity in the repository following the thermal pulse can be defined by a threshold temperature for MIC (T_{MIC}) below which a_W exceeds 0.96. Based on the data in Fig. 2, the value of T_{MIC} is 50 °C, 75 °C and 40 °C for the average, coolest, and hottest WP, respectively.

In the EBSCOM code, MIC can take two forms: MIC-enhanced general corrosion and MIC-induced localised corrosion. The DOE have reported a maximum of a twofold increase in the rate of general corrosion of Alloy 22 when exposed to microbial cultures and include this corrosion mechanism in WP degradation models [9]. Localised corrosion of Alloy 22 due to microbial activity has never been reported in the literature, but is a common form of MIC for other, less-corrosion-resistant, passive alloys [8]. Although the possibility for MIC-induced localised corrosion is included in EBSCOM, it is not implemented in the default version of the code and will not be until such time that there is reliable experimental evidence to indicate that microbes can induce the localised corrosion of Alloy 22.

4. Structure of the EBSCOM model

4.1. Definition of EBS failure

In the EBSCOM code, the performance of an individual WP is linked to the performance of the corresponding DS (Fig. 5). The model is structured around a series of flow charts, each of which determines either the parameters for a prediction (realisation) or the damage caused to each of the EBS components.

The DS is deemed to have failed if the entire wall thickness is consumed by general corrosion, there being little applied load in the absence of rock fall, or if the absorbed H concentration exceeds H_{CRIT}, whichever occurs first.

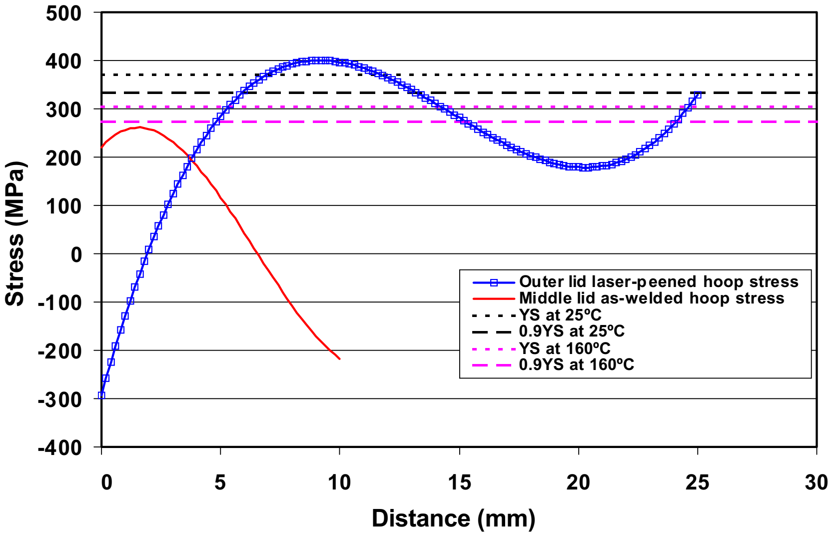

Fig. 4. Comparison of the depth dependence of the residual hoop stress for the laser-peened outer closure lid and the middle closure lid welds and EBSCOM criteria for the threshold stress for crack initiation.

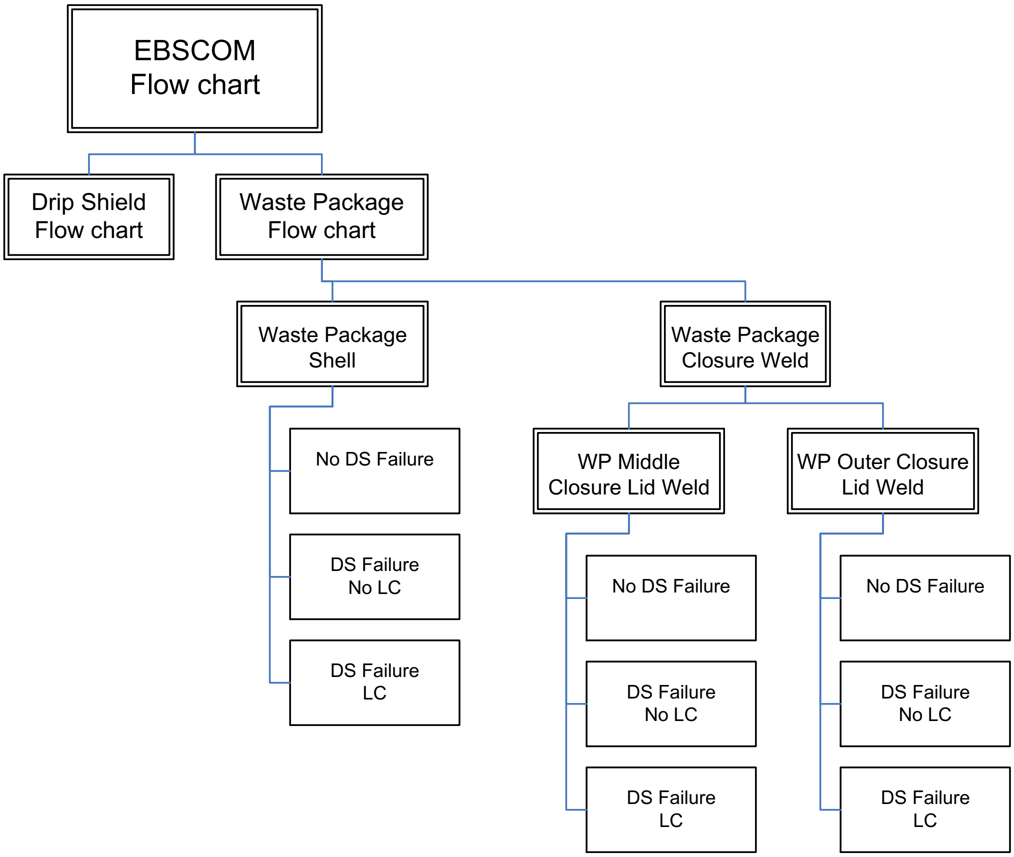

Fig. 5. Overall structure of the EBSCOM code.

The WP is deemed to have failed if either (a) the WP outer barrier is penetrated by a combination of general corrosion, localised corrosion, and MIC-enhanced general corrosion, or (b) both the outer and middle WP closure lid welds fail as a result of general corrosion, localised corrosion, MIC-enhanced general corrosion, and (for the outer closure weld only) SCC.

For both the DS and WP, a certain fraction of initial failures (10^{-4} [1]) is assumed to account for undetected manufacturing flaws and faulty emplacement of the DS.

Failure of the entire EBS is defined as the failure of a given WP and the corresponding DS.

4.2. Probabilistic aspects

A single run of the EBSCOM code comprises one million individual realisations. Each realisation is characterised by (Fig. 6):

1. the temperature at which an aqueous phase is stable on the WP and/or DS surface,
2. a particular temperature-time profile,
3. one of five possible environments (denoted Bins A–E),
4. a given probability that one or more of the EBS components is initially defected,
5. the temperature at which microbial activity is possible,
6. the general corrosion characteristics of the DS (including the rate of general corrosion of the DS at the reference temperature of 75 °C, the activation energy, factors for the effect of fluoride ions and the fraction of general corrosion supported by O_2 reduction),
7. the HIC characteristics of the DS (including the temperature-dependent hydrogen uptake efficiency and the critical hydrogen concentration),
8. the general corrosion characteristics of the WP shell (including the rate of general corrosion of the WP at the reference temperature of 75 °C and the activation energy),
9. the localised corrosion characteristics of the WP shell (including the threshold temperature for localised corrosion, the localised corrosion growth constant, activation energy, and time exponent),
10. the MIC GC enhancement factor, and
11. the specific corrosion characteristics of the closure lid welds (including the reduction factor for general corrosion of the laser-peened weld (outer closure lid only), the threshold temperature for localised corrosion of the weld, and the threshold stress for SCC initiation).

In this way, the EBSCOM code takes into account variability (in parameters such as the EBS temperature profile and the nature of the aqueous environment) and uncertainty (in parameters such as the rate of general corrosion of the WP and DS and the critical absorbed H concentration).

5. Predicted EBS lifetimes

Fig. 7 shows the predicted cumulative fraction of failed EBS components as a function of time up to 10^7 years for the nominal scenario. After 1,000,000 years, ~66% of DS are predicted to have failed, but only ~15% of WP. Failure of both the DS and WP is predicted to occur in only ~10% of the realisations. The times for the first corrosion failures are 40,000 years, 336,000 years, and 375,000 years for the DS, WP, and DS/WP combination, respectively.

Virtually all WP failures are the result of general corrosion of the shell. Because microbial activity in the repository is assumed to become possible as the temperature cools, the actual failure

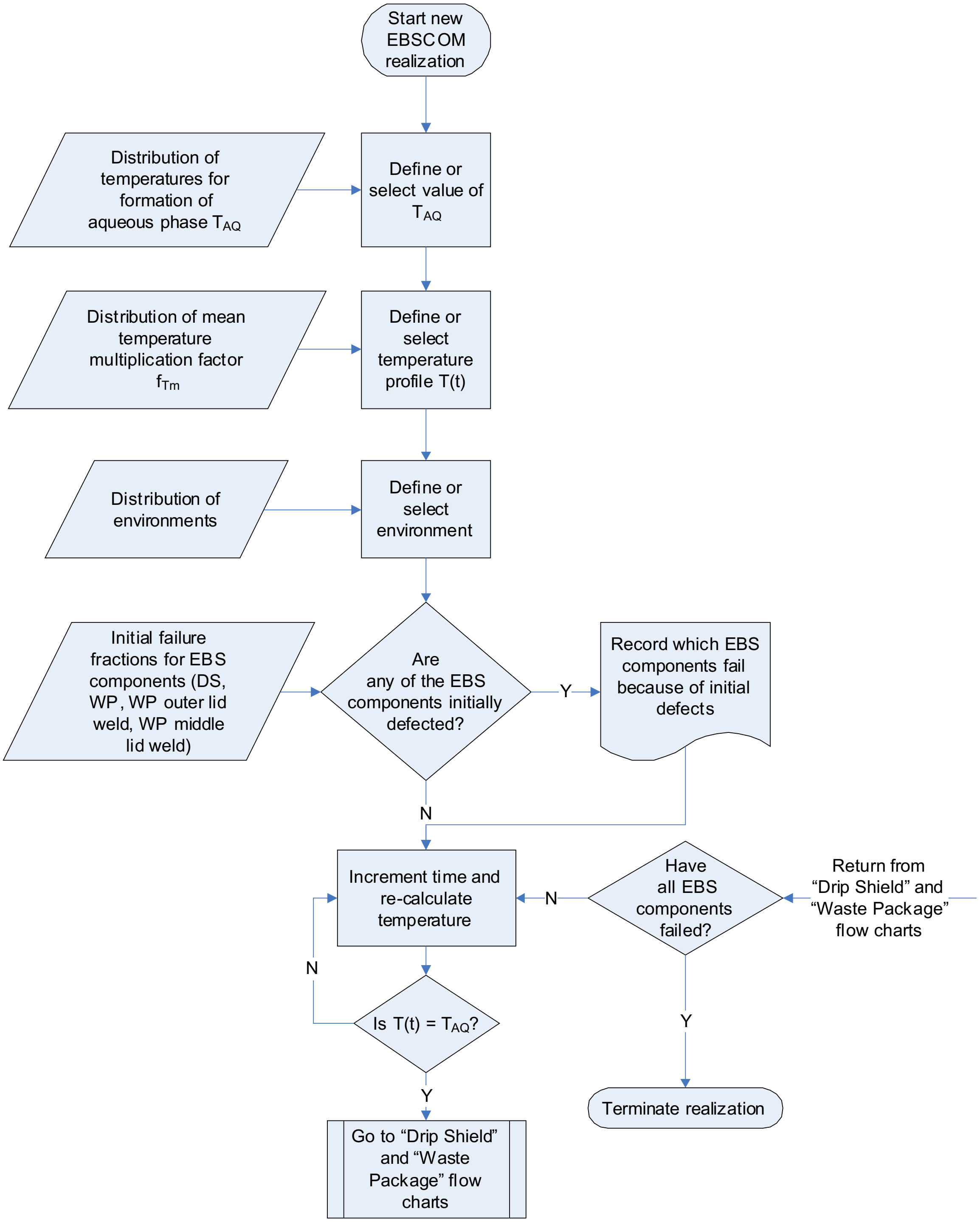

Fig. 6. Initial flow chart in each EBSCOM realisation.

mode is predicted to be microbiologically enhanced general corrosion. After 1,000,000 years there may be one failure of the lid system, most likely resulting from either (i) SCC of the outer closure lid weld combined with an initially failed middle lid or (ii) microbially enhanced general corrosion of the middle lid combined with an initially failed outer lid.

The relative lack of importance of SCC and localised corrosion as failure modes for the WP is a consequence of the non-conservative treatment of these processes in the EBSCOM code. In particular, the probability of failure by localised corrosion is low because the aqueous environment only supports localised attack in 1% of the realisations (corresponding to the frequency of the Bin A water). The low probability of SCC is the result of (i) the use of a threshold potential criterion for crack initiation, (ii) the use of a realistic threshold stress, and (iii) the reduced rate of general corrosion of the laser-peened outer closure lid weld (which extends the time until a sufficient tensile stress develops on the surface of the WP).

Both localised corrosion and SCC failure of the WP are possible under some circumstances. For example, a single realisation was performed for an initially failed DS in Bin A water (which supports localised corrosion). Waste package failure was predicted to result from localised corrosion of the shell after 1,680,000 years. Failure by SCC can occur, as described above, and is most likely for combi-

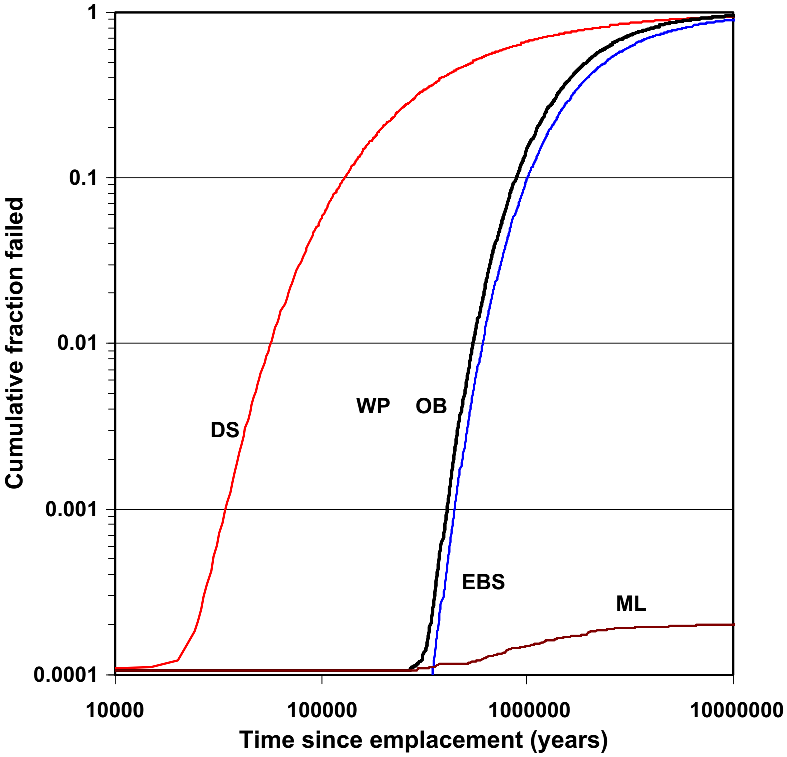

Fig. 7. Time dependence of the cumulative fraction of failed EBS components based on EBSCOM predictions for the nominal scenario.

Table 2
Times for various fractional failures of the EBS components based on EBSCOM predictions for the nominal scenario

CFF	DS	WP	EBS
0.0001	50 years	50 years	345,000 years
0.001	35,000	408,000	446,000
0.01	57,000	546,000	608,000
0.1	129,000	886,000	1,010,000
1	>2 × 10^7	>2 × 10^7	>2 × 10^7

nations of (i) a small reduction in the rate of general corrosion of the laser-peened weld material, (ii) a low threshold stress for crack initiation, and (iii) a threshold potential for SCC close to the lower bound of 0 mV_{SSC}. As a consequence of these numerous requirements, failure by SCC is predicted to be relatively uncommon, consistent with the results of recent experimental studies.

The major corrosion failure mode for the DS is general corrosion. Apart from a few HIC failures up to ~100,000 years, more than 99% of DS failures are due to general corrosion. General corrosion is predicted to be the predominant failure mode partly because of the assumptions that a fraction of the corrosion is supported by O_2 reduction and that previously absorbed H can be released as corrosion of the Ti matrix proceeds.

Table 2 lists the times for various values of the cumulative failure fraction (CFF) of the DS, WP, and entire EBS. For the DS and WP, the time for a fractional failure value of 0.0001 reflects the initially failed barriers. A CFF of 0.001 corresponds to ~11 failures. Thus, the vast majority of WP will remain intact for many hundreds of thousands of years.

Acknowledgement

This work was funded by the Electric Power Research Institute, John Kessler (Project Manager).

References

[1] Electric Power Research Institute, Evaluation of the Candidate High-Level Radioactive Waste Repository at Yucca Mountain Using Total System Performance Assessment, Phase 6, EPRI Report 1003031, Electric Power Research Institute, Palo Alto, CA, 2002.
[2] BSC, Multiscale Thermohydrologic Model, Bechtel SAIC Company Report to DOE, ANL-EBS-MD-000049 Rev 02, October 2004.
[3] BSC, Engineered Barriers System: Physical and Chemical Environment Model, Bechtel SAIC Company Report to DOE, ANL-EBS-MD-000033 Rev 02, February 2004.
[4] BSC, Technical Basis Document No. 6: Waste Package and Drip Shield Corrosion, Bechtel SAIC Company Report to DOE, Revision 1, December 2003.
[5] F. Hua, K. Mon, P. Pasupathi, G. Gordon, D. Shoesmith, in: Proceedings of the CORROSION/2004, National Association of Corrosion Engineers International, Houston, TX, Paper No. 04689, 2004.
[6] Z. Qin, D.W. Shoesmith, in: Proceedings of the NACE International Northern Region Eastern Conference, Ottawa, ON, NACE International, Houston, TX, September 2003.
[7] A.C. Lloyd, R.J. Schuler, J.J. Nöel, D.W. Shoesmith, F. King, Material Research Society, Symposium Proceedings, vol. 824, Materials Research Society, Warrendale, PA, 2004, p. 3.
[8] B. Little, P. Wagner, F. Mansfeld, Int. Mater. Rev. 36 (1991) 253.
[9] BSC, General Corrosion and Localized Corrosion of Waste Package Outer Barrier, Bechtel SAIC Company Report to DOE, ANL-EBS-MD-000003 Rev 02, October 2004.
[10] M.T. Peters, Status of Ongoing Testing, Presentation to the US Nuclear Waste Technical Review Board, 14 May 2003.
[11] R.B. Rebak, T.S.E. Summers, R.M. Carranza, Materials Research Society, Symposium Proceedings, vol. 608, Materials Research Society, Warrendale, PA, 2000, p. 109.
[12] M. Apted, F. King, D. Langmuir, R. Arthur, J. Kessler, J. Mater. 57 (2005) 43.
[13] G. Cragnolino, D.S. Dunn, Y.-M. Pan, Materials Research Society, Symposium Proceedings, vol. 807, Materials Research Society, Warrendale, PA, 2004, p. 435.
[14] BSC, Stress Corrosion Cracking of the Drip Shield, the Waste Package Outer Barrier, and the Stainless Steel Structural Material, Bechtel SAIC Company report to DOE, ANL-EBS-MD-000005 Rev 02, October 2004.
[15] A.D. Brown, Microbial Water Stress Physiology, John Wiley, Chichester, UK, 1990.
[16] F. King, M. Kolar, S. Stroes-gascoyne, P. Maak, Materials Research Society, Symposium Proceedings, vol. 807, Materials Research Society, Warrendale, PA, 2004, p. 811.